ISSN 0303-6812, Volume 61, Number 5

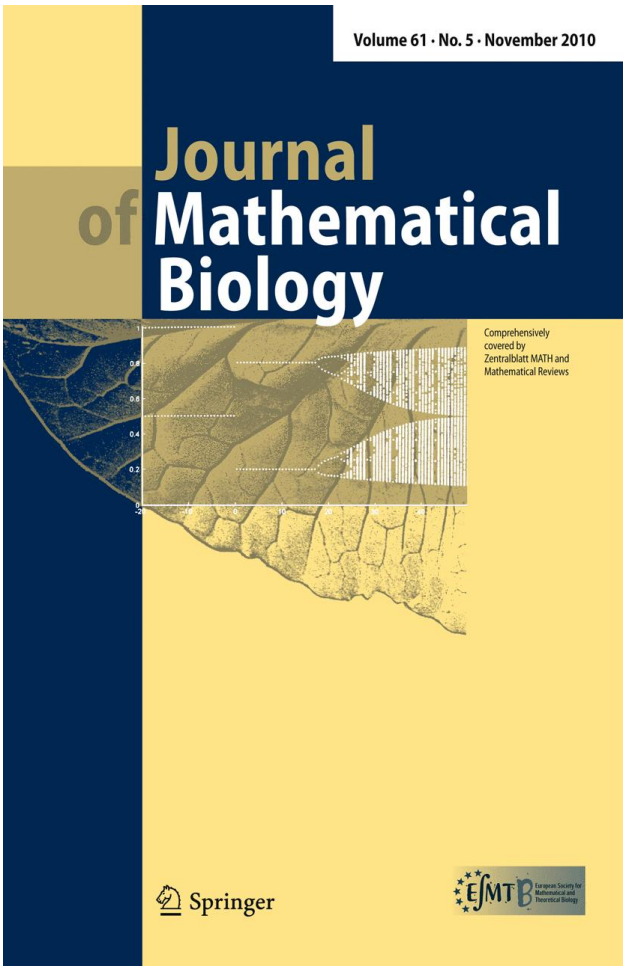

J. Math. Biol. (2010) 61:739–761
DOI 10.1007/s00285-009-0317-0

Mathematical Biology

Traveling wave solutions from microscopic to macroscopic chemotaxis models

Roger Lui · Zhi An Wang

Received: 14 January 2009 / Revised: 18 November 2009 / Published online: 27 December 2009

Abstract In this paper, we study the existence and nonexistence of traveling wave solutions for the one-dimensional microscopic and macroscopic chemotaxis models. The microscopic model is based on the velocity jump process of Othmer et al. (SIAM J Appl Math 57:1044–1081, 1997). The macroscopic model, which can be shown to be the parabolic limit of the microscopic model, is the classical Keller–Segel model, (Keller and Segel in J Theor Biol 30:225–234; 377–380, 1971). In both models, the chemosensitivity function is given by the derivative of a potential function, $\Phi(v)$, which must be unbounded below at some point for the existence of traveling wave solutions. Thus, we consider two examples: $\Phi(v) = \ln v$ and $\Phi(v) = \ln[v/(1-v)]$. The mathematical problem reduces to proving the existence or nonexistence of solutions to a nonlinear boundary value problem with variable coefficient on $\mathbb{R}$. The main purpose of this paper is to identify the relationships between the two models through their traveling waves, from which we can observe how information are lost, retained, or created during the transition from the microscopic model to the macroscopic model. Moreover, the underlying biological implications of our results are discussed.

Keywords Chemotaxis · Keller–Segel model · Traveling wave solutions · Potential functions · Chemical kinetics · Turning rate functions

Mathematics Subject Classification (2000) 35K57 · 35L60 · 35M10 · 92C17

R. Lui
Department of Mathematical Sciences, WPI, 100 Institute Road, Worcester, MA 01609, USA
e-mail: rlui@wpi.edu

Z. A. Wang (✉)
Institute for Mathematics and Its Applications, University of Minnesota,
Minneapolis, MN 55455, USA
e-mail: zhiwang@ima.umn.edu

1 Introduction

Chemotaxis is the directed movement of cells or organisms in response to chemical stimulus. It is a basic cellular process and plays an essential role in many important biological processes such as embryonic development, wound healing, and angiogenesis (Parent 2004). The mathematical study of chemotaxis was initiated with the pioneering work of Keller and Segel (1970), in which an advection-diffusion equation was proposed from a macroscopic (population-based) perspective to describe the aggregation of *Dictyostelium discoideum* in response to waves of cyclic adenosine monophosphate (cAMP). Their model is now commonly referred to as the Keller–Segel model. Since then, large amount of research have been performed and papers written on this and other related models (Horstmann 2003, 2004).

Modeling chemotaxis from a cell-based perspective was initiated by Patlak (1953), and later further developed by Alt (1980), and by Othmer et al. (1988). In Othmer et al. (1988), the authors derived a transport equation based on a velocity jump process to describe chemotactic movement of individual cells. It can be shown that the parabolic limit of the transport equation is the Keller–Segel model (Othmer and Hillen 2002). This provides support for the success of both Keller–Segel model and transport model in describing chemotactic movement from different perspectives. In this paper, the transport equation and the Keller–Segel model will be referred to as microscopic and macroscopic models, respectively.

The main result of this paper is the existence and nonexistence of traveling wave solutions for the one-dimensional microscopic and macroscopic models and their relationships. The experimental observation of traveling bands of bacterial chemotaxis was reported by Adler (1966). The mathematical modeling and analysis of traveling waves was first presented by Keller and Segel (1971b), which stimulated a flurry of activities by others [see Horstmann (2004) and references therein]. However all these theoretical results deal with the macroscopic model only. The result of traveling waves for the microscopic model was not reported to date. Since the macroscopic behavior is translated from the microscopic properties, we are motivated in this paper to study the traveling wave solutions for both macroscopic and microscopic chemotaxis model and examine how the traveling wave parameters in the microscopic model are translated to the macroscopic model. Biological implications of our results will be given at the end. In the rest of this section, we shall present the models that we study in this paper.

Let $u^+(t,x)$, $u^-(t,x)$ be the number densities of cells moving to the right and to the left at time t and position x, respectively. Let $v(t,x)$ be the chemical concentration that induces chemotactic cell movement. Suppose at random times, the cells change directions according to a Poisson process with intensity $\lambda^{\pm}$. Then, by assuming that the cells migrate with a constant speed s, $u^{\pm}$ and v satisfy the following system of equations:

$$\begin{cases} u_t^+ + s u_x^+ = -\lambda^+ u^+ + \lambda^- u^- \\ u_t^- - s u_x^- = \lambda^+ u^+ - \lambda^- u^- \\ v_t = D v_{xx} + g(u,v), \end{cases} \tag{1.1}$$

where $g(u, v)$ represents the kinetics between the chemical and the cells, and $u = u^+ + u^-$ is the total cell density. In general, $\lambda^{\pm}$, which we shall refer to as the turning rate functions, may depend on v, v_x and v_t. If $\lambda^{\pm}$ are independent of v_t, we follow Erban and Othmer (2004) and assume that they take the form

$$\lambda^{\pm}(v, v_x) = \lambda_0 \mp s\kappa\Phi(v)_x = \lambda_0 \mp s\kappa\varphi(v)v_x, \tag{1.2}$$

where λ_0 is the basal turning frequency when the cell is fully adapted to the signal and κ is related to the internal dynamics (signal transduction) of the cell. An example of $\kappa > 0$ given in Erban and Othmer (2004) is

$$\kappa = b_0 t_a/[(1 + 2\lambda_0 t_a)(1 + 2\lambda_0 t_e)] \tag{1.3}$$

where t_a and t_e are the adaptation and excitation time constants and $b_0 > 0$ is a scaling constant. $\Phi(v)$ and its derivative $\varphi(v)$ are called chemical potential and chemosensitivity functions, respectively (Hillen and Painter 2009). We assume that $\varphi(v) > 0$ in this paper. As a result, v acts as a chemoattractant which reduces the turning frequency for cells moving to the right when $v_x > 0$.

The parabolic limit mentioned above refers to the scalings $\xi = \varepsilon x, \tau = \varepsilon^2 t$ for system (1.1) and passing to the limit as $\varepsilon \downarrow 0$. Assuming that the turning rate functions are of the form (1.2), the parabolic limit of (1.1) is the Keller–Segel model:

$$\begin{cases} u_\tau = (du_\xi - \chi u\Phi(v)_\xi)_\xi \\ v_\tau = Dv_{\xi\xi} + g(u, v), \end{cases} \tag{1.4}$$

where d and χ are given by [see Erban and Othmer (2004)]

$$d = s^2/(2\lambda_0) \quad \text{and} \quad \chi = s^2\kappa/\lambda_0. \tag{1.5}$$

In a recent paper, Wang (2009), one of the authors (Wang) proved that the parabolic limit of (1.1) is also (1.4) when $\lambda^{\pm}$ also depends on the temporal gradient v_t of the chemical concentration.

During transition from the microscopic model to the macroscopic model, an important question is how much information in the microscopic model are lost, retained, or created in the macroscopic model. Inspired by this question, we examine the existence and nonexistence of traveling wave solutions for both models in this paper. We show that the existence of traveling waves solutions for the microscopic model is closely related to the value of the traveling wave speed c relative to the single cell speed s. We identify the relationship between the microscopic model and macroscopic model in terms of their traveling wave solutions. We then discuss the biological implications based on our results.

The organization of this paper is as follows. In Sect. 2, we formulate our problem, derive some conditions for the existence of traveling wave solutions, and state our main results in Theorem 2.5, Propositions 2.9 and 2.10. In Sect. 3, we prove Theorem 2.5, separating the proof into three cases: $c = 0$, $0 < c < s$, and $c = s$. Sections 4 and 5

contain the proofs of Proposition 2.9 and 2.10, respectively. In Sect. 6 we summarize our results and discuss the underlying biological implications.

2 Problem formulation and statements of main results

Throughout this paper, we shall assume that the turning-rate functions, $\lambda^{\pm}$, are of the form (1.2). Typical potential functions and their corresponding chemosensitivity functions are:

$$\begin{aligned}
&\Phi(v) = v, \quad \varphi(v) = 1 && \text{(Direct measurement)}\\
&\Phi(v) = \ln v, \quad \varphi = \frac{1}{v} && \text{(Logarithmic)}\\
&\Phi(v) = \frac{v}{K_d + v}, \quad \varphi(v) = \frac{K_d}{(K_d + v)^2} && \text{(Michaelis-Menten receptor kinetics)}\\
&\Phi(v) = \ln\left(\frac{v}{1 - v}\right), \quad \varphi(v) = \frac{1}{v(1 - v)} && \text{(Bounded signal).}
\end{aligned} \tag{2.1}$$

On the macroscopic level, the Direct Measurement potential function has been used extensively in the study of pattern formation of the Keller–Segel model (Hillen and Painter 2009), and first appeared in the paper by Rosen (1976). The Logarithmic potential function was first used by Keller and Segel (1971b), to describe the traveling band behavior of bacteria and subsequently used extensively by many other researchers [see Tindall et al. (2008) and the references therein]. The Michaelis-Menten Receptor Kinetics potential function was first applied by Lapidus and Schiller (1976) to fit the experimental observation of Brown and Berg (1974), where K_d represents the receptor-ligand binding dissociation rate constant. The Bounded Signal potential function is included for the study of traveling front solutions. This is the only potential function in (2.1) that is unbounded at two points.

On the microscopic level, the chemosensitivity function, $\varphi(v)$, characterizes the sensing mechanism employed by cells to detect and transduce signal. The Direct Measurement chemosensitivity function represents linear response and signal-independent sensitivity. The other chemosensitivity functions in (2.1) represent nonlinear sensing mechanisms that are signal dependent. The Logarithmic chemosensitivity function applies to the situation where the cells are highly sensitive at low concentration of the signal and become less sensitive as signal concentration increases due to adaptation. The Michaelis-Menten Receptor Kinetics chemosensitivity function was motivated by a receptor-signal binding model which postulates that at high signal concentration, the receptors on the cell surface may be fully occupied and the cell is unable to further resolve a gradient (Lapidus and Schiller 1976). The Bounded Signal chemosensitivity function postulates high sensitivity at the low and high concentrations of the signal. This kind of sensing mechanism has not been addressed in the literature and we propose it here to study the existence of traveling pulse-front solutions in the case where the traveling wave speed coincide with the individual cell speed (see Sect. 4). There are some other sensing mechanisms that are summarized in Tindall et al. (2008) and

Hillen and Painter (2009), but the study of each of such mechanisms will go beyond the scope of this paper.

2.1 Microscopic model

Let $u = u^+ + u^-$ and let $j = s(u^+ - u^-)$ be the total density flux. Then system (1.1) can be written as

$$\begin{cases} u_t + j_x = 0 \\ j_t + s^2 u_x = -F_1 u - F_2 j \\ v_t = D v_{xx} + g(u, v), \end{cases} \tag{2.2}$$

where

$$F_1 = s(\lambda^+ - \lambda^-) \quad \text{and} \quad F_2 = \lambda^+ + \lambda^-.$$

Traveling wave solutions of (2.2) are special solutions of the form $\tilde{u}(z)$, $\tilde{j}(z)$, $\tilde{v}(z)$ where $z = x - ct$ and c is a constant called the wave speed. Substituting F_1, F_2 into (2.2), we have

$$\begin{cases} -cu_z + j_z = 0 \\ -cj_z + s^2 u_z = 2s^2 \kappa u \varphi(v) v_z - 2\lambda_0 j \\ -cv_z = D v_{zz} + g(u, v), \end{cases} \tag{2.3}$$

where the tildes on top of u, j, v have been deleted for notational convenience. We assume zero flux boundary conditions $j(\pm\infty) = 0$. From the first equation of (2.2), we have

$$\int_{\mathbb{R}} u(t, x)dx = \int_{\mathbb{R}} u_0(x)dx = m_0 > 0.$$

Since $u \geq 0$, we have $u(\pm\infty) = 0$, $j = cu$, and system (2.3) may be simplified to the following traveling wave system:

$$\begin{cases} (s^2 - c^2)u_z = -2c\lambda_0 u + 2s^2 \kappa u \Phi(v)_z \\ -cv_z = D v_{zz} + g(u, v). \end{cases} \tag{2.4}$$

Note that we can recover $u^\pm$ from the formulas $u^\pm = (u \pm j/s)/2$. We impose the following boundary conditions on u and v:

$$u(\pm\infty) = 0 \quad \text{and} \quad v(\pm\infty) = v_\pm, \tag{2.5}$$

where $v_\pm$ are finite. If $v_\pm = 0$, then we call the solutions of (2.4) and (2.5) traveling pulse-pulse solutions. If $v_- = 0$ and $v_+ > 0$, then we call the solutions traveling pulse-front solutions.

From the relation $j = cu$, we have

$$\frac{u^+(z) - u^-(z)}{u^+(z) + u^-(z)} = \frac{c}{s}. \tag{2.6}$$

Since $u^\pm \geq 0$, (2.6) implies that $-s \leq c \leq s$. If $c^2 \neq s^2$, we integrate the first equation in (2.4) to obtain

$$u(z) = C_0 e^{-2\sigma(\lambda_0 cz - s^2\kappa\Phi(v))}, \tag{2.7}$$

where $\sigma = 1/(s^2 - c^2)$ and $C_0 > 0$ is the constant of integration. Since $u(-\infty) = 0$, we have $\Phi(v_-) = \lim_{z\to-\infty}\Phi(v(z)) = -\infty$. If $c^2 = s^2$, then $\Phi(v)_z = \varphi(v)v_z = \lambda_0/c\kappa$. Thus, $\varphi(v_\pm)$ are unbounded. Among the potential functions given in (2.1), only the Logarithmic and Bounded Signal potential functions satisfy these conditions with $v_- = 0$. Therefore, we only consider these two potential functions for the microscopic model in this paper.

2.2 Macroscopic model

The traveling wave system for the macroscopic model (1.4) is

$$\begin{cases} -cU = dU_z - \chi U\Phi(V)_z \\ -cV_z = DV_{zz} + g(U, V), \end{cases} \tag{2.8}$$

where we have assumed that $U(-\infty) = 0$, $U'(-\infty) = 0$, and $\Phi(V)_z$ is bounded. Let d, χ be defined by (1.5). Then (2.8) can be written as

$$\begin{cases} s^2U_z = -2c\lambda_0 U + 2s^2\kappa U\Phi(V)_z \\ -cV_z = DV_{zz} + g(U, V). \end{cases} \tag{2.9}$$

This is the same as (2.4) except that $s^2 - c^2$ is replaced by s^2 on the left. We impose the following boundary conditions on U and V:

$$U(\pm\infty) = 0 \quad \text{and} \quad V(\pm\infty) = V_\pm. \tag{2.10}$$

An equation similar to (2.7) can be derived with σ replaced by $\tilde{\sigma} = 1/s^2$. Hence, we also only consider the Logarithmic and Bounded Signal potential functions with $V_- = 0$ for the macroscopic model in this paper.

Remark 2.1 If $(u(z), v(z))$ is a solution of (2.4) with speed c, then $(u(-z), v(-z))$ is also a solution of (2.4) with speed $-c$. Similar statement can be made for the macroscopic model (2.9). Hence, for the proof of the existence of traveling wave solutions with speed c, it suffices to assume that $c \geq 0$. Also, it is obvious from the traveling wave systems (2.4) and (2.9) that translations of a traveling wave solution is also a traveling wave solution.

Remark 2.2 If we substitute (2.7) into the second equation in (2.4), we obtain the following boundary value problem

$$Dv_{zz} + cv_z + g(C_0 e^{-2\sigma(\lambda_0 cz - s^2\kappa\Phi(v))}, v) = 0, \quad v(\pm\infty) = v_\pm. \tag{2.11}$$

This boundary value problem also holds for the macroscopic traveling wave system (2.9) by changing σ to $\tilde{\sigma}$. Clearly, not much can be said about (2.11) without knowing $g(u, v)$. Therefore, we assume throughout this paper that g is linear; i.e. $g(u, v) = \alpha u - \beta v$. This form of kinetics has not been considered in the study of the traveling waves before, but it has been used extensively to study global existence and pattern formations of the Keller–Segel model, Hillen and Painter (2009). However, this form was not included in the forms studied by Horstmann and Stevens in Horstmann and Stevens (2004). In this paper, we shall find conditions on α, β such that traveling wave solutions exist.

Remark 2.3 Suppose $v(z)$ is a solution of (2.11) with $g(u, v) = \alpha u - \beta v$. Let τ satisfy $e^{2\sigma\lambda_0 c\tau} = C_0$. Then $v(z + \tau)$ is a solution of (2.11) corresponding to $C_0 = 1$. Therefore, without loss of generality, we shall assume that $C_0 = 1$ in (2.11) throughout this paper.

Remark 2.4 Suppose $g(u, v) = \alpha u - \beta v$ in (2.11). Then $g(0, v_\pm) = -\beta v_\pm = 0$. Hence, traveling pulse-front solutions can exist only if $\beta = 0$.

We now state the main results of this paper. For convenience, we let

$$k = 2\sigma\lambda_0 c \quad \text{and} \quad r = 2\sigma s^2\kappa$$

for the rest of this paper. In the following theorems, the microscopic (macroscopic) model refers to traveling wave Eqs. (2.4) and (2.5) [(2.9) and (2.10)]. Traveling wave solutions mean either traveling pulse-pulse solutions or traveling pulse-front solutions.

Theorem 2.5 *Let* $\Phi(v) = \ln v$ *and let* $g(u, v) = \alpha u - \beta v$. *Then*

(i) *for the case* $c = 0$, *the microscopic and macroscopic models are identical. Traveling pulse-pulse solutions of speed zero exist if and only if* $D > 0, 2\kappa > 1, \alpha > 0$ *and* $\beta > 0$. *Traveling pulse-front solutions of speed zero do not exist.*

(ii) *for the case* $0 < c < s$, *it holds that*

  (a) *if* $D = 0$, *then traveling pulse-pulse solutions of speed* c *exist for the microscopic model if and only if* $r \geq 1, \alpha < 0$, *and* $\beta < 0$. *Traveling pulse-front solutions of speed c exist if and only if* $r \geq 1, \alpha < 0$ *and* $\beta = 0$,

  (b) *if* $D > 0$, *then traveling pulse-pulse solutions of speed* c *exist for the microscopic model if* $r > 1, \alpha < 0, \beta < 0$, *and* $2\sqrt{-\beta D} \leq c < s$. *Traveling pulse-front solutions of speed c exist if* $r > 1, \alpha < 0$ *and* $\beta = 0$. *Same results in* (ii) *hold for the macroscopic model with* r *replaced by* $\tilde{r} = 2\kappa = \chi/d$.

(iii) *for the case* $c = s$, *traveling wave solutions of speed* c *do not exist for the microscopic model. For the macroscopic model, it holds that*

(a) *if $D = 0$, then the macroscopic model admits traveling pulse-pulse solutions of speed c if and only if $2\kappa \geq 1, \alpha < 0$, and $\beta < 0$. It also admits traveling pulse-front solutions of speed c if and only if $2\kappa \geq 1, \alpha < 0$ and $\beta = 0$,*

(b) *if $D > 0$, then the macroscopic model has traveling pulse-pulse solutions of speed c if $2\kappa > 1, \alpha < 0, \beta < 0$ and $c \geq 2\sqrt{-\beta D}$. It also admits traveling pulse-front solutions of speed c if $2\kappa > 1, \alpha < 0$ and $\beta = 0$.*

Remark 2.6 For the microscopic model to be biologically meaningful, the turning rate functions, $\lambda^{\pm}$, should be nonnegative. Since the proof of Theorem 2.5 does not require the conditions under which the turning rate functions are nonnegative, we present the conditions for the non-negativity of turning rate functions separately in Proposition 2.10.

Remark 2.7 The microscopic model is only valid if $0 \leq c \leq s$ since population wave speed cannot exceed individual cell speed. However, for the macroscopic model, which comes from (2.8), c can be arbitrarily large. In fact, we shall see in Sect. 3.3 that Theorem 2.5(iii)(a) and (b) are valid even if $c > s$. In addition, from Theorem 2.5(iii), the microscopic model does not possess traveling wave solutions when $c = s$. Hence, the most biologically relevant case is when $0 \leq c < s$.

Remark 2.8 In our model, the presence of the chemoattractant causes individual cells to change directions and the population to slow down and travel at speed c. Our analysis is divided into the cases of zero diffusion ($D = 0$) and nonzero diffusion ($D \neq 0$) for the chemical. The former applies to haptotaxis, or gliding movement of myxobacteria towards slime trails (Othmer and Stevens 1997), and the latter applies to the diffusible chemical which is the case in most situations (Horstmann 2003). In Theorem 2.5, one of the main conditions for the existence of traveling wave solutions for the microscopic model is $r > 1$, or equivalently, $2\kappa > 1 - (c/s)^2$. Since κ is related to the internal dynamics of the cell, this condition means that the chemoattractant needs to have a suitably strong impact on the cells before the population movement can develop into a traveling wave. In the kinetic term $g(u, v)$ for the chemical, the conditions $\alpha < 0, \beta \leq 0$ mean that the chemoattractant is consumed by cells ($\alpha < 0$) to balance the exponential growth of the chemical ($\beta < 0$). For the macroscopic model, the equivalent condition is $\chi > d$, which means that the chemotactic effect has to overcome the diffusion effect before traveling waves can exist. Some species, such as *Dictyostelium discoideum* and *E. Coli*, can secret their own chemicals for chemotaxis (Eisenbach 2004). In such a case, both α and β are positive, and Theorem 2.5(i) says that standing wave solutions can exist if $D > 0$ and κ is suitably large.

It can be shown from (2.7) that if $c = s$, then $\Phi(v_+) = \infty$. Hence, there is no traveling wave solution if $\Phi(v) = \ln v$ but there may be traveling pulse-front solution for the Bounded Signal potential function with $v_+ = 1$. The following result verifies this.

Proposition 2.9 *Let $\Phi(v) = \ln[v/(1-v)]$ for $0 < v < 1$ and let $g(u, v) = \alpha u - \beta v$. Suppose $c = s$. Then traveling pulse-front solutions for the microscopic model with*

$v_- = 0, v_+ = 1$ exist if and only if $\alpha < 0, \beta = 0$ and $s^2 > D\lambda_0/\kappa$. In addition, the turning rate functions, $\lambda^\pm$, are nonnegative for all parameter values. For the macroscopic model, assuming that $D = 0$, traveling pulse-front solutions with $V_- = 0, V_+ = 1$ exist if $\alpha < 0, \beta = 0$ and $2\kappa \geq 1$.

The following proposition addresses the non-negativity of turning rate functions $\lambda^\pm$ for the biologically most significant case $0 \leq c < s$ and traveling pulse-pulse solutions (i.e. $\beta \neq 0$). Note that traveling wave solutions of the microscopic model do not exist if $\Phi(v) = \ln v$ and $c = s$. The proposition and proof can be readily extended to the case of traveling pulse-front solutions (i.e. $\beta = 0$) with obvious modifications.

Proposition 2.10 *Let the hypotheses of the microscopic model in Theorem 2.5*(i)*, Theorem 2.5*(ii)(a) *and Theorem 2.5*(ii)(b) *be satisfied for cases* (i), (ii)(a) *and* (ii)(b) *below, respectively. Then*

(i) *for the case $c = 0$, $\lambda^\pm$ are nonnegative on $\mathbb{R}$ if $\lambda_0 \geq s\kappa\sqrt{\beta/D}$.*
(ii) *for the case $0 < c < s$,*
  (a) *if $D = 0$, it holds that*
    (1) *if $r > 1$, then $\lambda^\pm$ are positive on $\mathbb{R}$ if and only if $-\kappa\beta/\lambda_0 < c/s < 2\kappa - 1$.*
    (2) *if $r = 1$, then λ^+ is always negative near $-\infty$.*
  (b) *if $D > 0$ and $\kappa > 1$, then $\lambda^\pm$ are positive on $\mathbb{R}$ if*

$$\frac{c}{s} < \frac{D\lambda_0(\kappa - 1)}{s^2\kappa^2 + D\lambda_0(\kappa - 1)}. \tag{2.12}$$

Remark 2.11 From the proof of Proposition 2.10, condition (2.12) ensures that the turning rate functions, $\lambda^\pm$, are positive at a local minimum. In case $D = 0$, such a condition is no longer needed because $\lambda^\pm$ are monotone. This fact does not seem to be true when $D > 0$ but we cannot find a numerical example to show that (2.12) is actually necessary.

3 Proof of Theorem 2.5

3.1 Case $c = 0$

In this case, (2.4) and (2.9) are identical so we only consider (2.4). Equation (2.7) becomes $u(z) = v^{2\kappa}(z)$. Hence, $v_\pm = 0$ and there is no pulse-front solution. The boundary value problem (2.11) becomes

$$Dv_{zz} + \alpha v^{2\kappa} - \beta v = 0, \quad v(\pm\infty) = 0. \tag{3.1}$$

It is clear that there is no traveling wave solution if $D = 0$. If $\alpha\beta \leq 0$, then v is either concave or convex on $\mathbb{R}$ which is inconsistent with $v(z) \geq 0$ and $v(\pm\infty) = 0$. Hence, $\alpha\beta > 0$. We write (3.1) as a first-order system:

$$\begin{cases} v_z = w \\ w_z = \frac{1}{D}(\beta v - \alpha v^{2\kappa}). \end{cases} \tag{3.2}$$

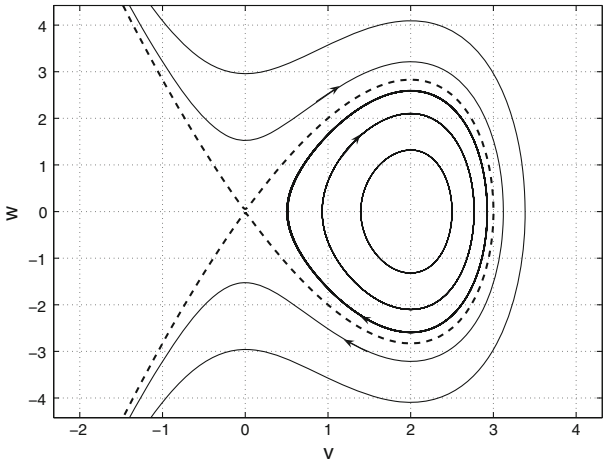

Fig. 1 Phase portrait of (3.2) for the case $c = 0$ with $D = 1$, $\alpha = 1$, $\beta = 1$, and $\kappa = 1$. The *dashed curve* is the homoclinic orbit corresponding to the traveling pulse solution for v

If $2\kappa < 1$, then the right side of the above system is not differentiable at the origin. If $2\kappa = 1$, then (3.1) is linear. It can be solved explicitly and shown to have no nonnegative solution. Thus, $2\kappa > 1$. System (3.2) has two steady states $(0, 0)$ and $(\delta, 0)$, where $\delta^{2\kappa-1} = \beta/\alpha > 0$. The eigenvalues of the linearized matrices at $(0, 0)$ and $(\delta, 0)$ are $\pm\sqrt{\beta/D}$ and $\pm\sqrt{\beta(1-2\kappa)/D}$, respectively. If $\beta < 0$, then $(0, 0)$ is a center and there is no trajectory connecting $(\delta, 0)$ to $(0, 0)$ or itself that lies entirely in the region $v > 0$. Therefore, $\beta > 0$. The origin is then a saddle and $(\delta, 0)$ is a center. System (3.2) is a Hamiltonian system with

$$H(v, w) = \frac{1}{2}w^2 - \frac{\beta}{2D}v^2 + \frac{\alpha}{(2\kappa+1)D}v^{2\kappa+1} \tag{3.3}$$

which is constant on any trajectory. Figure 1 shows the trajectory (dashed line) of a traveling wave solution for v connecting the unstable manifold to the stable manifold at the origin. This completes the proof of Theorem 2.5(i).

3.2 Case $0 < c < s$

3.2.1 Microscopic model

The boundary value problem (2.11) becomes

$$Dv_{zz} + cv_z + \alpha e^{-kz}v^r - \beta v = 0, \quad v(-\infty) = 0, \ \ v(\infty) = v_+. \tag{3.4}$$

Proof of Theorem 2.5(ii)(a) *when* $D = 0$.

We first consider traveling pulse-pulse solutions with $v_+ = 0$.

$r < 1$: Let $f_1 = -\beta/c$ and let $f_2(z) = -\alpha \exp(-kz)/c$. Then (3.4) becomes $v_z + f_1 v = f_2(z)v^r$. The change of variable $y = v^{1-r}$ transforms the above equation into $y_z + (1-r)f_1 y = (1-r)f_2(z)$. The general solution of this equation is $y(z) = C_1 e^{(1-r)\beta z/c} + C_2 e^{-kz}$ where $C_1 > 0$ and

$$C_2 = \frac{(1-r)\alpha}{kc + \beta(1-r)}. \tag{3.5}$$

Therefore, v is given by

$$v(z) = \left(C_1 e^{(1-r)\beta z/c} + C_2 e^{-kz}\right)^{\frac{1}{1-r}}. \tag{3.6}$$

If $r < 1$, then $v(\infty) \to \infty$ if $\beta > 0$ and $v(-\infty) \to \infty$ if $\beta \leq 0$. Hence, there is no traveling wave solution in this case.

$r = 1$: Equation (3.4) is linear and can be solved to yield

$$v(z) = C_3 \exp\left(\frac{\beta}{c}z + \frac{\alpha}{kc}e^{-kz}\right) \tag{3.7}$$

$$u(z) = C_3 \exp\left(\left(\frac{\beta}{c} - k\right)z + \frac{\alpha}{kc}e^{-kz}\right) \tag{3.8}$$

where (2.7) has been used to obtain $u(z)$. It is easy to see that $v(\pm\infty) = u(\pm\infty) = 0$ if and only if $\alpha < 0$ and $\beta < 0$. Hence, traveling pulse-pulse solutions exist for this case.

$r > 1$: The calculations in the case $r < 1$ and (3.6) are still valid. Note that the outermost exponent in (3.6) is negative. If $\beta > 0$, then $v(z) \to \infty$ as $z \to \infty$. If $\beta = 0$, then $v(z) \to C_1^{1/(r-1)} > 0$ as $z \to \infty$. So in both cases, v cannot be a traveling pulse solution. If $\beta < 0$, then $v(z) \to 0$ as $z \to \infty$. If $C_2 > 0$, then $v(z) \to 0$ as $z \to -\infty$ so v is a traveling pulse. The condition $C_2 > 0$ is equivalent to $\alpha < 0$. Thus, if both α and β are negative, then $v(\pm\infty) = 0$. Now u is given by

$$u(z) = e^{-kz} v^r(z), \tag{3.9}$$

which implies that $u(\infty) = 0$. From (3.6), $u(z) \sim e^{kz/(r-1)}$ as $z \to -\infty$. (Here, $f(x) \sim g(x)$ as $x \to x_0$, where x_0 is an extended real number, means that $\lim_{x\to x_0} f(x)/g(x) = \text{constant} \neq 0$.) Thus, $u(-\infty) = 0$ and traveling pulse-pulse solutions exist. Numerical example of a traveling pulse-pulse solution is shown in Fig. 2a and the corresponding turning rate functions are shown in Fig. 2b.

We now consider traveling pulse-front solutions with $v_+ > 0$.

From Remark 2.4, we have $\beta = 0$ and v satisfies the equation $cv_z = -\alpha e^{-kz} v^r$. If $r = 1$, then

$$v(z) = C_4 \exp\left(\frac{\alpha}{kc}e^{-kz}\right)$$

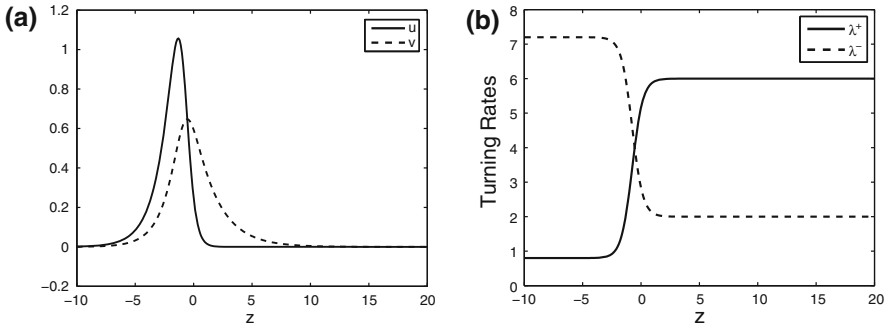

Fig. 2 **a** Traveling wave solutions of the microscopic model with $\Phi(v) = \ln v$, $g(u, v) = \alpha u - \beta v$, and $D = 0$, $\beta \neq 0$. **b** Graphs of turning rate functions $\lambda^{\pm}$ corresponding to the traveling wave solutions shown in (**a**). Parameter values are: $\alpha = -1$, $\beta = -1$, $s = 4$, $c = 2$, $\lambda_0 = 4$, and $\kappa = 1$

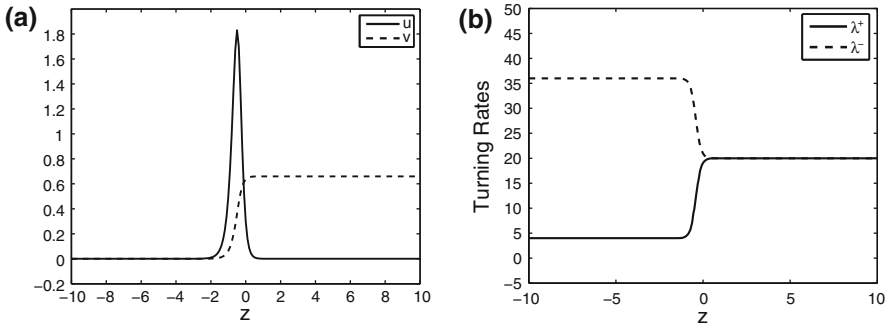

Fig. 3 **a** Traveling wave solutions of the microscopic model with $\Phi(v) = \ln v$, $g(u, v) = \alpha u - \beta v$, and $D = 0$, $\beta = 0$. **b** Graphs of turning rate functions $\lambda^{\pm}$ corresponding to the traveling wave solutions shown in (**a**). Parameter values are: $\alpha = -1$, $s = 4$, $c = 2$, $\lambda_0 = 10$, and $\kappa = 1$

where $C_4 > 0$. In order for $v(-\infty) = 0$, α must be negative. Then $v(\infty) = C_4$ and $v(z)$ is a traveling front solution. If $r \neq 1$, then (3.6) becomes

$$v(z) = \left[v_+^{1-r} + \frac{\alpha(1-r)}{ck} e^{-kz} \right]^{\frac{1}{1-r}}.$$

In order for $v(-\infty) = 0$, we must have $r > 1$, and in order that $v(z) > 0$, we must have $\alpha < 0$. Thus, traveling pulse-front solutions exist if and only if $r \geq 1$, $\alpha < 0$ and $\beta = 0$. The proof of Theorem 2.5(ii)(a) with $D = 0$ is complete. Numerical example of a traveling pulse-front solutions is shown in Fig. 3a and the corresponding turning rate functions are shown in Fig. 3b.

Proof of Theorem 2.5(ii)(b) *when* $D > 0$ By dividing (3.4) throughout by D and relabeling the constants c/D, s/D, α/D, β/D, λ_0/D as c, s, α, β, λ_0, respectively, we may assume that $D = 1$. Note that the last assumption in the Theorem 2.5 is stated with respect to the unscaled c, s, α, β and λ_0. If $r = 1$, Eq. (3.4) is linear with variable coefficient and cannot be solved explicitly. We do not discuss this case here.

We first consider traveling pulse-pulse solutions with $v_+ = 0$.
Let $w = ve^{\mu z}$ and let

$$\mu = \frac{-k}{r-1} \quad \text{where } r \neq 1. \tag{3.10}$$

Then w satisfies the equation

$$w_{zz} + (-2\mu + c)w_z + (\mu^2 - c\mu - \beta)w = -\alpha w^r. \tag{3.11}$$

Rewriting (3.11) as a first order system, we have

$$\begin{cases} w' = \varrho \\ \varrho' = -a\varrho - bw - \alpha w^r, \end{cases} \tag{3.12}$$

where $a = -2\mu + c$ and $b = \mu^2 - c\mu - \beta$. There are two equilibria: $(w_1, \varrho_1) = (0, 0)$, which always exists, and $(w_2, \varrho_2) = ([-b/\alpha]^{1/(r-1)}, 0)$, which exists if $-b/\alpha > 0$. If $0 < r < 1$, the right side of (3.12) is not differentiable at the origin. Thus, we assume that $r > 1$ which implies that $\mu < 0$ and $a > 0$. It can be shown that if (w_2, ϱ_2) does not exist, then there cannot be a trajectory connecting the unstable manifold to the stable manifold at the origin. Therefore, no traveling pulse solutions exist in that case.

Let us assume that $-b/\alpha > 0$ and (w_2, ϱ_2) exists. Let J_1 and J_2 be the linearized matrices at these two equilibria, respectively. Then the eigenvalues of matrix J_1 are

$$\xi_1 = \frac{-a - \sqrt{a^2 - 4b}}{2}, \quad \xi_2 = \frac{-a + \sqrt{a^2 - 4b}}{2},$$

and the eigenvalues of J_2 are

$$\eta_1 = \frac{-a - \sqrt{a^2 + 4b(r-1)}}{2}, \quad \eta_2 = \frac{-a + \sqrt{a^2 + 4b(r-1)}}{2}.$$

If $b < 0$, then $\xi_1 < 0 < \xi_2$. If there is a trajectory connecting $(0, 0)$ to (w_2, ϱ_2), then $v(z) \sim (w_2 + Ce^{\eta_2 z})e^{-\mu z}$ as $z \to \infty$ which means $v_+ = \infty$ since $\mu < 0$ and $\mathrm{Re}(\eta_2) < 0$. Thus we assume that $b > 0$ and consequently $\alpha < 0$. If $\beta > 0$, then Eq. (3.4) is not satisfied at the maximum of $v(z)$. Therefore, both α and β are negative. Since $a^2 - 4b = c^2 + 4\beta$, we have $\xi_1 < \xi_2 < 0$ if $c^2 \geq -4\beta$ which is one of our hypotheses. Also, $\eta_1 < 0 < \eta_2$. We now show that there is a trajectory connecting the unstable manifold of (w_2, ϱ_2) to $(0, 0)$. This trajectory will give us traveling pulse-pulse solutions.

Consider the parabolic equation

$$w_t = w_{xx} + h(w) \tag{3.13}$$

where $h(w) = w(b + \alpha w^{r-1})$. We look for traveling wave solution $\tilde{w}(z) = \tilde{w}(x - \hat{c}t)$ satisfying the boundary conditions $\tilde{w}(-\infty) = w_2$ and $\tilde{w}(\infty) = 0$. The traveling wave

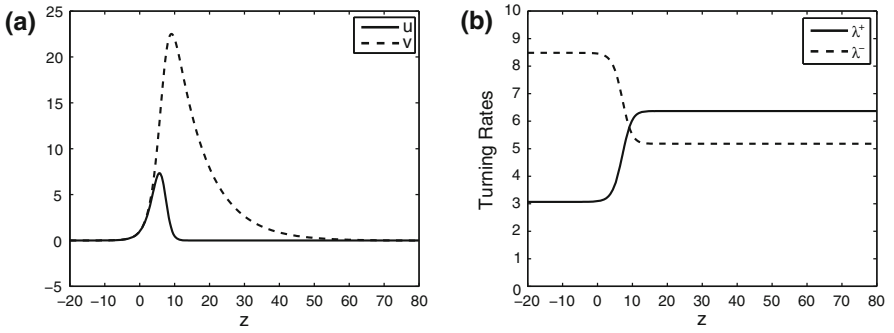

Fig. 4 **a** Traveling wave solutions of the microscopic model with $\Phi(v) = \ln v$, $g(u, v) = \alpha u - \beta v$, and $D = 1$, $\beta \neq 0$. **b** Graphs of turning rate functions $\lambda^{\pm}$ corresponding to the traveling waves shown in (**a**). Parameter values are: $\alpha = -1$, $\beta = -0.125$, $s = 4$, $c = 1.25$, $\lambda_0 = 5.8$, and $\kappa = 1.35$

equation is $\hat{w}_{zz} + \hat{c}\hat{w}_z + h(\hat{w}) = 0$. Since $h(0) = h(w_2) = 0$, $h(w) > 0$ in $(0, w_2)$, $h'(0) = b > 0$, $h'(w_2) = (1-r)b < 0$ and $h''(w) = \alpha r(r-1)w^{r-2} < 0$, Eq. (3.13) is a Fisher-KPP type equation. It is known that [see Kolmogorov et al. (1937)] there exist traveling front solutions if and only if $\hat{c} \geq 2\sqrt{h'(0)}$ which translates to $c^2 \geq -4\beta$. In other words, if this condition holds, then there is a decreasing function w satisfying Eq. (3.11) such that $w(-\infty) = w_2$ and $w(\infty) = 0$. The only questions left are whether $v(\pm\infty)$ and $u(\pm\infty)$ equal to zero.

From above, $v(z) = w(z)e^{-\mu z}$, $\eta_2 > 0$ and $\mu < 0$. Therefore, $v(z) \sim (w_2 + Ce^{\eta_2 z})e^{-\mu z} \to 0$ as $z \to -\infty$. On the other hand, $v(z) \sim e^{(\xi_2 - \mu)z}$ as $z \to \infty$, which approaches zero as $z \to \infty$ if $\xi_2 - \mu < 0$. This last condition is equivalent to $a^2 - 4b < c^2$ which is satisfied because $\beta < 0$.

Turning to $u(z)$, from (3.9), we have

$$u(z) \sim (w_2 + Ce^{\eta_2 z})^r e^{-(\mu r + k)z} \quad \text{as } z \to -\infty.$$

From (3.10), $\mu r + k = \mu$. Since $\eta_2 > 0, r > 1$ and $\mu < 0$, it follows that $u(z) \sim (w_2 + Ce^{\eta_2 z})^r e^{-\mu z} \to 0$ as $z \to -\infty$. Similarly,

$$u(z) \sim e^{(\xi_2 r - \mu)z} \quad \text{as } z \to \infty.$$

Since $r > 1$ and $\xi_2 < 0$, we have $\xi_2 r - \mu < \xi_2 - \mu < 0$. Therefore, $u(z) \to 0$ as $z \to \infty$. The proof of the first part of the proposition is complete. Numerical example of a traveling pulse-pulse solution (u, v) is shown in Fig. 4a and the corresponding turning rate functions are shown in Fig. 4b.

We now consider traveling pulse-front solutions with $v_+ > 0$.

From Remark 2.4, we have $\beta = 0$. One observes from the above proof that $\xi_2 = \mu$ if $\beta = 0$ so that $v(z)$ approaches a constant as $z \to \infty$. Therefore traveling pulse-front solutions exist for the microscopic model if $r > 1, \alpha < 0$ and $\beta = 0$. Numerical example of a traveling pulse-front solution is shown in Fig. 5a and the corresponding turning rate functions are shown in Fig. 5b. The proof of Theorem 2.5(ii)(b) with $D > 0$ is complete.

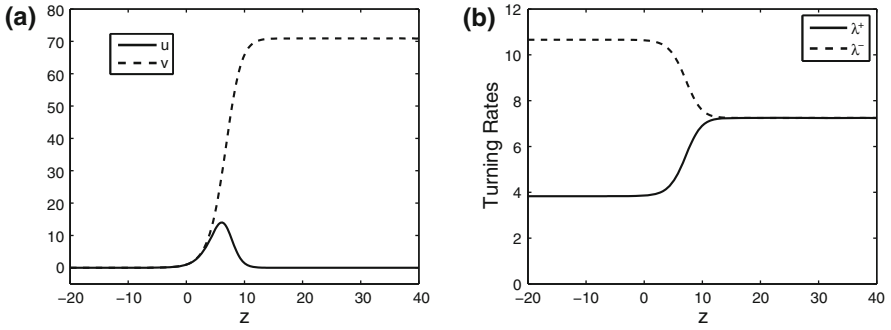

Fig. 5 **a** Traveling wave solutions of the microscopic model with $\Phi(v) = \ln v$, $g(u, v) = \alpha u - \beta v$, and $D = 1$, $\beta = 0$. **b** Graphs of turning rate functions $\lambda^{\pm}$ corresponding to the traveling waves shown in (**a**). Parameter values are $\alpha = -1$, $s = 4$, $c = 1$, $\lambda_0 = 7.25$, and $\kappa = 1.4$

3.2.2 Macroscopic model

From the first equation of the traveling wave system (2.9), we have

$$U(z) = e^{-2\tilde{\sigma}\lambda_0 cz} V^{2\kappa}(z)$$

where $\tilde{\sigma} = 1/s^2$. Thus the above results on microscopic model also hold for macroscopic model with r replaced by $\tilde{r} = 2\kappa = \chi/d$.

Remark 3.1 From the above analysis, we see that the microscopic and macroscopic models have traveling pulse-pulse solutions if $r \geq 1$ and $\tilde{r} \geq 1$, respectively. Since $r > \tilde{r}$, in case $r > 1 > \tilde{r}$, traveling pulse-pulse solutions exist for the microscopic model but not for the macroscopic model.

3.3 Case $c = s$

3.3.1 Microscopic model

We have shown in Sect. 2 that traveling wave solutions do not exist for the microscopic model if $c > s$. Now we examine the case $c = s$. Since u is not identically zero, let (a, b) be the maximum interval where $u > 0$. Here, a, b may be extended real numbers and if a or b is finite, then u must vanish there by continuity. From the first equation of (2.4), we have

$$v(z) = C_0 e^{\lambda_0 z/s\kappa} \quad \text{in } (a, b). \tag{3.14}$$

From the second equation of (2.4), we have

$$u(z) = -\frac{\left(D\left(\frac{\lambda_0}{s\kappa}\right)^2 + s\left(\frac{\lambda_0}{s\kappa}\right) - \beta\right) C_0 e^{\lambda_0 z/s\kappa}}{\alpha} \quad \text{in } (a, b). \tag{3.15}$$

From (3.15), $\alpha \neq 0$ for otherwise, u is undefined on (a, b). In other words, if $\alpha = 0$, then the second equation of (2.4) does not contain u and cannot be used to find u. From (3.15), u cannot vanish anywhere which implies that $a = -\infty$ and $b = \infty$. In other words, $u > 0$ on $\mathbb{R}$. It then follows from (3.14) that $v(\infty) = v_+ = \infty$. Since v_+ is finite, no traveling wave solution exists for the Logarithmic potential function when $c = s$.

3.3.2 Macroscopic model

Integrating the first equation in (2.9), we have

$$U(z) = e^{-\tilde{k}z} V^{2\kappa}(z)$$

where $\tilde{k} = 2\lambda_0 c/s^2$. Substituting this into the second equation of (2.9), we have

$$DV_{zz} + sV_z + \alpha e^{-\tilde{k}z} V^{2\kappa} - \beta V = 0, \quad V(-\infty) = 0, \ V(\infty) = V_+. \tag{3.16}$$

Comparing (3.16) with (3.4), we can conclude Theorem 2.5(iii) directly from the results obtained in the previous subsections. From the above results, we see that there are significant differences between the two models when $c = s$.

4 Proof of Proposition 2.9

Let $\Phi(v) = \ln[v/(1-v)]$ for $0 < v < 1$. Then $\varphi(v) = \Phi'(v) = 1/[v(1-v)]$, $\Phi^{-1}(v) = 1/(1+e^{-v})$. Let $c = s$. For the microscopic model, using an argument similar to that presented in Sect. 3.3, one can show that $u > 0$ on $\mathbb{R}$ so that $\Phi(v)_z = \lambda_0/s\kappa$. Integrating and from above, we have

$$v(z) = \frac{1}{1 + C_6 e^{-\lambda_0 z/s\kappa}}, \tag{4.1}$$

where $C_6 > 0$. Hence, $v_+ = 1, v_- = 0$ and $v(z)$ is a traveling front. Let $g(u) = \alpha u - \beta v$. Then the equation $Dv_{zz} + cv_z + \alpha u - \beta v = 0$ can be solved explicitly to yield

$$u(z) = \frac{\xi(z)}{\alpha}\left\{-s + \frac{D\lambda_0}{s\kappa}\left(1 - \frac{2C_6}{C_6 + e^{\lambda_0 z/s\kappa}}\right)\right\} + \frac{\beta}{\alpha} v(z) \tag{4.2}$$

where

$$\xi(z) = v_z(z) = \frac{\frac{\lambda_0}{s\kappa} C_6 \exp\left(-\frac{\lambda_0}{s\kappa} z\right)}{\left(1 + C_6 \exp\left(-\frac{\lambda_0}{s\kappa} z\right)\right)^2}.$$

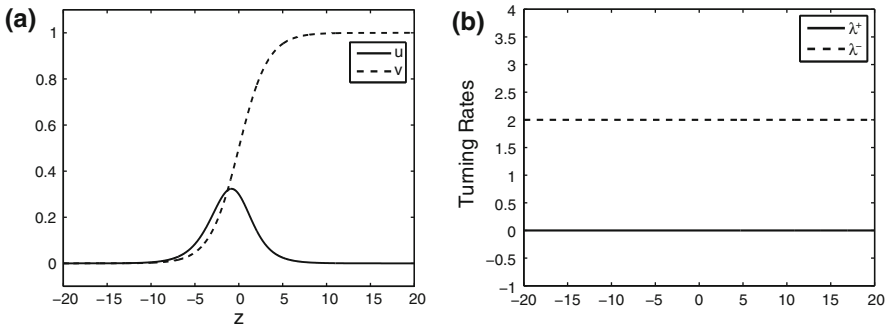

Fig. 6 **a** Traveling pulse-front solutions of the microscopic model for the case $c = s$ where $\Phi(v) = \ln[v/(1-v)]$ and $g(u,v) = \alpha u - \beta v$. **b** Graphs of turning rate functions correspond to the traveling pulse-front solutions in (**a**). Parameter values are $\alpha = -2, \beta = 0, C_6 = 1, \lambda_0 = 1, s = 1, D = 1$ and $\kappa = 2$.

Since $\xi(\pm\infty) = 0$, we must have $\beta = 0$ in order for $u(\pm\infty) = 0$. The term inside the parenthesis in (4.2) increases from -1 to 1 as z increases from $-\infty$ to ∞. Since $\xi(z) > 0$, we must have $\alpha < 0$ and $s^2 > D\lambda_0/\kappa$ in order that $u(z) > 0$. If these conditions are satisfied, then (u, v) is a traveling pulse-pulse solution. A numerical example is shown in Fig. 6a.

Next we show the non-negativity of the turning rate functions $\lambda^{\pm} = \lambda_0 \mp s\kappa\Phi(v)_z = \lambda_0 \mp s\kappa v_z/[v(1-v)]$. Let $\zeta = C_6 e^{-\lambda_0 z/s\kappa}$. Then from (4.1), $v = 1/(1+\zeta)$ and

$$\frac{v_z}{v(1-v)} = \frac{\frac{\lambda_0}{s\kappa}\zeta}{(1+\zeta)^2}\frac{1}{\frac{1}{1+\zeta}\left(1-\frac{1}{1+\zeta}\right)} = \frac{\lambda_0}{s\kappa}.$$

Thus, $\lambda^{\pm} = \lambda_0 \mp s\kappa(\frac{\lambda_0}{s\kappa}) = \lambda_0 \mp \lambda_0 \geq 0$ with $\lambda^+ = 0$ and $\lambda^- = 2\lambda_0$. Graphs of the turning rate functions corresponding to the traveling wave solutions in Fig. 6a are shown in Fig. 6b.

For the macroscopic model and Bounded Signal potential function, one cannot express V in terms of Φ^{-1}. Solving the first equation of (2.9), we have

$$U(z) = e^{-2\lambda_0 z/s}\left(\frac{V}{1-V}\right)^{2\kappa} \tag{4.3}$$

where we have scaled the constant of integration to one by translation. Substituting this into the second equation of (2.9), the resulting differential equation is too complex to be analytically tractable. Therefore, we assume that $D = 0$ and $g(u,v) = \alpha u$. From the second equation of (2.9), we have

$$V_z = -\frac{\alpha}{s}\left(\frac{V}{1-V}\right)^{2\kappa} e^{-2\lambda_0 z/s}. \tag{4.4}$$

If $\alpha > 0$, then $V_z < 0$ and no traveling wave solutions with $V(-\infty) = 0$ exist. If $\alpha < 0$, we assume that $2\kappa \geq 1$ and let $W = V/(1-V)$. Then $V = W/(1+W)$ and

$$\frac{W_z(z)}{(1+W(z))^2} = -\frac{\alpha}{s} W(z)^{2\kappa} e^{-bz} \tag{4.5}$$

where $b = 2\lambda_0/s > 0$. Let $W(z)$ be defined implicitly by

$$\int_{W(z)}^{\infty} \frac{1}{\xi^{2\kappa}(1+\xi)^2} d\xi = -\frac{\alpha}{bs} e^{-bz}.$$

It is clear that $W(z)$ satisfies (4.5). Since $2\kappa \geq 1$, the function $1/[\xi^{2\kappa}(1+\xi)^2]$ is not integrable at the origin and integrable at infinity. Thus, $W(-\infty) = 0$ and $W(\infty) = \infty$. This implies that $V_- = 0$ and $V_+ = 1$ and $V(z)$ is a traveling front solution for the macroscopic model. Note that if $2\kappa = 1$, then $W(z)$ can be expressed in terms of the Lambert W function. The proof of the proposition is complete.

Remark 4.1 For the microscopic model, v is determined only by the potential function and u can then be determined from the second equation of (2.4). However, for the macroscopic model, U is given in terms of V by (4.3) through the potential function and V is then determined from the second equation of (2.4). Hence, there are fundamental differences between the traveling wave solutions of the microscopic and macroscopic models in the case $c = s$.

5 Proof of Proposition 2.10

Recall that $k = 2\sigma\lambda_0 c$, $r = 2\sigma s^2\kappa$, $\sigma = 1/(s^2 - c^2)$, and α and β are negative when $0 < c < s$. In the following, we let $\theta(z) = v_z(z)/v(z)$ and $\eta = c/s \in (0,1)$. Since $\Phi(v) = \ln v$, the turning rate function $\lambda^{\pm}(z) = \lambda_0 \mp s\kappa\theta(z)$. Note that $\kappa > 1$ implies the condition $2\kappa > 1 + \eta$ which in turn implies the condition $r > 1$.

Proof of case (i) *when* $c = 0$.

When $c = 0$, the existence of traveling wave solutions has been proved in Sect. 3.1. From (3.2), $\lambda^{\pm} = \lambda_0 \mp s\kappa w/v$ where $w = v_z$. Since $(v(z), w(z)) \to (0,0)$ as $|z| \to \infty$, the Hamiltonian (3.3) is zero along the traveling wave trajectory. That is $\frac{1}{2}w^2 - \frac{\beta}{2D}v^2 + \frac{\alpha}{(2\kappa+1)D}v^{2\kappa+1} = 0$, which can be rearranged as

$$\frac{w^2}{v^2} = \frac{\beta}{D} - \frac{2\alpha}{(2\kappa+1)D} v^{2\kappa-1}.$$

Since $v \geq 0$, we have $\left|\frac{w}{v}\right| \leq \sqrt{\frac{\beta}{D}}$. From above, $\lambda^{\pm} \geq \lambda_0 - s\kappa\sqrt{\frac{\beta}{D}} \geq 0$ if $\lambda_0 \geq s\kappa\sqrt{\frac{\beta}{D}}$. The proof of case (i) of Proposition 2.10 is complete.

Proof of case (ii)(a) *when* $0 < c < s$ *and* $D = 0$. Suppose $r > 1$. Then v is given by (3.6),

$$\theta(z) = \frac{1}{c(1-r)} \frac{C_1\beta(1-r)e^{\beta(1-r)z/c} - cC_2ke^{-kz}}{C_1e^{\beta(1-r)z/c} + C_2e^{-kz}} \tag{5.1}$$

and

$$\theta'(z) = \frac{C_1C_2(\beta(1-r)/c + k)^2 e^{(\beta(1-r)/c-k)z}}{(1-r)(C_1e^{\beta(1-r)z/c} + C_2e^{-kz})^2} < 0. \tag{5.2}$$

Hence, $\theta(\infty) < \theta(z) < \theta(-\infty)$. From (5.1), one has

$$\theta(-\infty) = -\frac{k}{1-r} = -\frac{2\sigma\lambda_0 c}{1-r} > 0 \quad \text{and} \quad \theta(+\infty) = \frac{\beta}{c} < 0.$$

In order for $\lambda^{\pm} \geq 0$ on $\mathbb{R}$, it is necessary and sufficient that

$$\lambda_0 + \frac{s\kappa\beta}{c} > 0 \quad \text{and} \quad \lambda_0\left(1 - \frac{2\sigma s\kappa c}{r-1}\right) > 0. \tag{5.3}$$

The first inequality in (5.3) is equivalent to $\eta > -\kappa\beta/\lambda_0$. The second inequality in (5.3) simplifies to $2s\kappa c < 2s^2\kappa - s^2 + c^2$. Dividing by s^2, rearranging, and dividing by $1 - \eta$, we have $\eta < 2\kappa - 1$.

If $r = 1$, then v is given by (3.7) which yields

$$\theta(z) = \frac{\beta}{c} - \frac{\alpha}{c}e^{-kz}.$$

Since $\alpha < 0$, $\theta(z)$ is decreasing, $\theta(-\infty) = \infty$, and $\lambda^+ = \lambda_0 - s\kappa\theta(z)$ is always negative near $-\infty$. The proof of Proposition 2.10(ii)(a) is complete.

Proof of case (ii)(b) *when* $0 < c < s$ *and* $D > 0$.

Recall that in the proof of Theorem 2.5(ii)(b), we have scaled the parameters c, s, α, β and λ_0 (except κ) by dividing them by D so that we may assume that $D = 1$.

Suppose λ^+ or λ^- has a local minimum at z^*. Then from the definitions of $\lambda^{\pm}$, $\theta_z(z^*) = 0$. Since $\theta = v_z/v$, we have $\theta_z = v_{zz}/v - \theta^2$, and the equation in (3.4) becomes

$$\theta_z + \theta^2 + c\theta + \alpha w^{r-1} - \beta = 0,$$

where $w = ve^{\mu z}$ and $\mu = -k/(r-1) < 0$. At z^*, we have $(\theta^*)^2 + c\theta^* + \alpha(w^*)^{r-1} - \beta = 0$, where $\theta^* = \theta(z^*)$ and $w^* = w(z^*)$. Therefore,

$$\theta^* = \frac{-c \pm \sqrt{c^2 + 4\beta - 4\alpha(w^*)^{r-1}}}{2}.$$

From the proof of Theorem 2.5(ii)(b), $w(z)$ decreases from $w_2 = (-b/\alpha)^{1/(r-1)}$ to 0. Since $\alpha < 0$, the term inside the above radical sign is less than $c^2+4\beta-4\alpha(-b/\alpha) = c^2 + 4\beta + 4(\mu^2 - c\mu - \beta) = (2\mu - c)^2$. Since $\mu < 0$, we have $-c + \mu \le \theta^* \le -\mu$ and

$$\lambda^{\pm}(z^*) \ge \min\{\lambda_0 + s\kappa(-c+\mu), \lambda_0 + s\kappa\mu\}. \tag{5.4}$$

The first term on the right of (5.4) is positive if $\lambda_0 - s\kappa k/(r-1) > s\kappa c$, which is same as

$$\lambda_0 \left(\frac{2\sigma s^2\kappa - 1 - 2s\kappa\sigma c}{2\sigma s^2\kappa - 1} \right) > s\kappa c.$$

Since $\sigma = 1/(s^2 - c^2)$, the above inequality is same as

$$\lambda_0 \left(\frac{(1-\eta)(2\kappa - 1 - \eta)}{2\kappa - 1 + \eta^2} \right) > s\kappa c. \tag{5.5}$$

Since $2\kappa > 1 + \eta$, the function $(2\kappa - 1 - \eta)/(2\kappa - 1 + \eta^2)$ is decreasing on $(0, 1)$ so that

$$\frac{\kappa - 1}{\kappa} < \frac{2\kappa - 1 - \eta}{2\kappa - 1 + \eta^2} < 1. \tag{5.6}$$

Therefore, a sufficient condition for (5.5) to hold is

$$\lambda_0 > \frac{\eta s^2 \kappa^2}{(1-\eta)(\kappa - 1)}. \tag{5.7}$$

Solving for η in (5.7) and dividing c, s, λ_0 by D to return to their unscaled forms, we obtain (2.12). The condition that the second term on the right of (5.4) is positive is the same as $2\sigma s^2\kappa - 1 - 2s\kappa\sigma c > 0$. This is equivalent to $2\kappa > 1 + \eta$ which is satisfied because $\kappa > 1$. Therefore, from (5.4), $\lambda^{\pm}(z^*)$ cannot be negative if $\kappa > 1$ and (2.12) hold.

Besides the critical points, we also have to check the behavior of $v_z(z)/v(z)$ as $|z| \to \infty$. Recall that in the proof of Theorem 2.5(ii)(b), we have shown that $v(z) \sim e^{(\xi_2 - \mu)z}$ as $z \to \infty$. Therefore, $v_z(z)/v(z) \to \xi_2 - \mu = (-c + \sqrt{c^2 + 4\beta})/2 < 0$ as $z \to \infty$ and we require that

$$\lambda_0 > s\kappa \left(\frac{c - \sqrt{c^2 + 4\beta}}{2} \right). \tag{5.8}$$

This condition is implied by (5.7) since the right side of (5.7) is greater than $s\kappa c$. Multiplying the right side of (5.8) by $c + \sqrt{c^2 + 4\beta}$, rearranging, and dividing λ_0, β, s, c by D to return them to their unscaled forms, we obtain

$$\eta + \sqrt{\eta^2 + \frac{4\beta D}{s^2}} > \frac{-2\kappa\beta}{\lambda_0}.$$

If we let $D \to 0$, above becomes $\lambda_0 + \kappa\beta/\eta > 0$ which is one of the conditions in the case $D = 0, r > 1$. To continue, $v(z) \sim (w_2 + Ce^{\eta_2 z})e^{-\mu z}$ as $z \to -\infty$. Since $\eta_2 > 0$, we have $v_z(z)/v(z) \to -\mu = k/(r-1)$ as $z \to -\infty$. Therefore, we also need $\lambda_0 - s\kappa k/(r-1) > 0$. This simplifies to $2\kappa > 1 + \eta$ which follows from the condition $\kappa > 1$. Hence, the conditions $\kappa > 1$ and (2.12) already ensure that $\lambda^{\pm} > 0$ at $\pm\infty$. The proof of Proposition 2.10 is complete.

6 Summary and biological implications

In this paper, we studied the existence and nonexistence of traveling wave solutions for the microscopic and macroscopic chemotaxis models. The macroscopic model was obtained from the microscopic model by passing to the parabolic limit. We assumed that the potential function is of the Logarithmic or Bounded Signal type. We found that proving the existence of traveling wave solutions is equivalent to proving the existence of solutions to a nonlinear second-order ($D > 0$), or first-order ($D = 0$), boundary value problem on $\mathbb{R}$.

Because of symmetry, we only need to consider the case when the traveling wave speed c is nonnegative. The results for the Logarithmic potential function is as follows. If $c = 0$, then the microscopic and macroscopic models are the same, and we give a sufficient and necessary condition for the existence of traveling pulse-pulse solutions. No traveling pulse-front solutions exist in this case. For $0 < c < s$, both models admit traveling wave solutions that are qualitatively similar. For $c \geq s$, traveling wave solutions do not exist for the microscopic model but exist for the macroscopic model. In summary, the larger the c, the more different are the traveling wave solutions of the two models. Since cell population consists of individual cells and so population wave speed cannot exceed individual cell speed, we conclude that the relevant biological situation for the existence of traveling wave solutions is when $0 \leq c \leq s$.

When $0 < c < s$ and $D = 0$, a necessary condition for the existence of traveling wave solutions for the microscopic model is $2\rho\kappa \geq 1$, where κ is a measurement of the internal dynamics of the cell and $\rho = s^2/(s^2 - c^2)$. This condition is replaced by $2\kappa \geq 1$ for the macroscopic model whose traveling wave solutions can exist for all values of c. Therefore, traveling wave solutions are preserved during the transition from the microscopic model to the macroscopic model if $2\rho\kappa > 2\kappa > 1$ but may be lost if c, s and κ are such that $2\rho\kappa > 1 > 2\kappa$. This quantitative characterization indicates that the transition of traveling waves from the microscopic model to the macroscopic model may depend on the strength of internal dynamics, i.e., the value of internal parameter κ. When $0 < c < s$ and $D > 0$, the analysis is more involved and we gave a sufficient condition for the existence of traveling wave solutions [see Theorem 2.5ii(b)].

For $c = s$ and the Bounded Signal potential function, we showed that there are some fundamental differences between the traveling wave solutions of the microscopic and macroscopic models (see Remark 4.1). This implies that when the cell population

traveling speed is identical to the individual cell speed, there might be dramatic changes in the transition from individual to collective behavior of cells.

The chemical kinetics in this paper is assumed to be linear, i.e. $g(u, v) = \alpha u - \beta v$. Except when $c = 0$, two other necessary conditions for the existence of traveling wave solutions are $\alpha < 0$ and $\beta \leq 0$. If $\beta < 0$, traveling wave solutions are pulse-pulse solutions and when $\beta = 0$, traveling wave solutions are pulse-front solutions. When $c = 0$, it requires that $\alpha > 0, \beta > 0$. In the formulation of our model in Sect. 2, we assumed that the chemical is the chemoattractant. The condition $\alpha < 0$ means that cells consume the chemical (e.g. food) and the condition $\alpha > 0$ corresponds to the endogenous chemotaxis meaning that the cells, such as *E. Coli*, secrete the chemical themselves.

Consider a traveling wave solution of (2.4) where Φ is the Logarithmic potential function and the turning rate functions $\lambda^{\pm} = \lambda_0 \mp s\kappa\Phi(v)_z$ are nonnegative on $\mathbb{R}$. Since $\Phi'(v) = \varphi(v) = 1/v \to \infty$ as $v \to 0$, low chemical concentration dominates the chemotactic response. This appears to be a puzzle as stated in Hillen and Painter (2009). However, assuming that $u > 0$ and dividing the first equation of (2.4) by $-us^2$, we obtain after some algebra the equation

$$\left(\frac{c}{s} - 1\right)\left[\left(\frac{c}{s} + 1\right)\frac{u_z}{u} - \frac{2}{s}\lambda_0\right] = \frac{2}{s}\lambda^+ \geq 0.$$

Since u decreases to zero as $z \to \infty, u_z/u \leq 0$ as $z \to \infty$. The above equation implies that $c \leq s$. In other words, if traveling wave solutions exist and the turning rate functions are nonnegative, then the macroscopic speed cannot exceed the biological limit. We have given conditions when the turning rate functions are nonnegative in Proposition 2.10. This also implies that $\Phi(v)_z = v_z/v$ is bounded on $\mathbb{R}$ for otherwise the turning rate functions will be negative at some point. Thus the Logarithmic potential function is an appropriate form for studying traveling wave solutions of chemotaxis models. This choice has already been used successfully by Keller and Segel (1971b), to interpret traveling band behavior of bacteria observed in experiment. Our study here also supports such a choice of potential functions. However, we do not expect our explanation to be true in general if the solutions are not traveling wave solutions.

Acknowledgments The authors are grateful to the referees for their valuable comments which greatly improve the exposition of this manuscript. This research was supported in part by the Institute for Mathematics and its Applications (IMA) with funds provided by the National Science Foundation. Zhi An Wang was supported by the IMA postdoctoral fellowship.

References

Adler J (1966) Chemotaxis in bacteria. Science 153:708–716

Alt W (1980) Biased random walk model for chemotaxis and related diffusion approximation. J Math Biol 9:147–177

Brown D, Berg H (1974) Temporal stimulation of chemotaxis in *Escherichia coli*. Proc Natl Acad Sci 71(4):1388–1392

Eisenbach M (2004) Chemotaxis. Imperial College Press, London

Erban R, Othmer H (2004) From individual to collective behavior in bacterial chemotaxis. SIAM J Appl Math 65(2):361–391

Hillen T, Painter K (2009) A user's guide to pde models for chemotaxis. J Math Biol 58:183–217
Horstmann D (2003) From 1970 until present: the Keller–Segel model in chemotaxis and its consequences I. Jahresberichte der DMV 105(3):103–165
Horstmann D (2004) From 1970 until present: the Keller–Segel model in chemotaxis and its consequences II. Jahresberichte der DMV 106(2):51–69
Horstmann D, Stevens A (2004) A constructive approach to travelling waves in chemotaxis. J Nonlinear Sci 14:1–25
Keller EF, Segel LA (1970) Initiation of slime mold aggregation viewd as an instability. J Theor Biol 26:399–415
Keller EF, Segel LA (1971a) Model for chemotaxis. J Theor Biol 30:225–234
Keller EF, Segel LA (1971b) Traveling bands of chemotactic bacteria: a theoretical analysis. J Theor Biol 30:235–248
Kolmogorov AN, Petrovskii IG, Piskunov NS (1937) A study of the equation of diffusion with inrcease in the quantity of matter, and its application to a biological problem. Bjol Moskovskovo Gos Univ 17:1–72
Lapidus R, Schiller R (1976) Model for the chemotactic response of a bacterial population. Biophys J 16:779–789
Othmer H, Dunbar SR, Alt W (1988) Models of dispersal in biological systems. J Math Biol 26:263–298
Othmer H, Hillen T (2002) The diffusion limit of transport equations II: chemotaxis equations. SIAM J Appl Math 62(4):1122–1250
Othmer H, Stevens A (1997) Aggregation, blowup and collapse: the ABC's of taxis in reinforced random walks. SIAM J Appl Math 57:1044–1081
Parent CA (2004) Making all the right moves: chemotaxis in neutrophils and dictyostelium. Curr Opin Cell Biol 16:4–13
Patlak CS (1953) Random walk with persistence and external bias. Bull Math Biophys 15:311–338
Rosen D (1976) Existence and nature of band solutions to generic chemotactic transport equations. J Theor Biol 59:243–246
Tindall MJ, Maini PK, Porter SL, Armitage JP (2008) Overview of mathematical approaches used to model bacterial chemotaxis II: bacterial populations. Bull Math Biol 70(6):1570–1607
Wang ZA (2009) Connections between microscopic and macroscopic models for chemotaxis. SIAM J Math Anal (in review)